

Nargalam M. Hasanguliyeva , Ninel V. Shakunova* , Yuriy N. Litvishkov 

Institute of Catalysis and Inorganic Chemistry named after acad. M. Nagiyev of Ministry of Science and Education of Republic of Azerbaijan, Baku, Azerbaijan

(*Corresponding author's e-mail: nqasanquliyeva@mail.ru)

Microwave Solid-Phase Synthesis of Ni-Co Ferrites and their Activities in Liquid-Phase Oxidation of *m*-Xylene

In this paper, the activity of mono- and di-substituted cobalt and nickel ferrites prepared by microwave solid-phase synthesis was studied in the reaction of liquid-phase oxidation of *m*-xylene to *m*-toluic acid. It was established that among the tested samples, the di-substituted ferrites of spinel structure with the composition of $\text{Ni}_{0.6}\text{Co}_{0.4}\text{Fe}_2\text{O}_4$ have the shortest induction period and the highest initial rate of oxygen absorption. In order to clarify the role of the active surface of the $\text{Ni}_{0.6}\text{Co}_{0.4}\text{Fe}_2\text{O}_4$ catalyst and the volumetric conversions of *m*-xylene in the nucleation stage of primary xylol radicals, the dependence of the induction period. Furthermore the rate of oxygen absorption was investigated as a function of the time of introduction of the inhibitor into the oxidized *m*-xylene at different ratios of the total size of the heterogeneous surface to the volume of *m*-xylene loaded into the reactor (S/V). The dependence of the selectivity of the process to the targeted product, *m*-toluic acid, on the specific surface area of the catalyst samples was established and it was shown that selectivity to the by-product, *m*-methylbenzyl alcohol, increased and selectivity to *m*-toluic acid decreased in the case of cobalt ferrite with a relatively low specific surface area. It was shown that at the first stage reaction (5–10 min.), i.e., in conditions of an as yet undeveloped radical chain reaction, in the presence of disubstituted ferrites of the composition ($\text{Ni}_{1-x}\text{Co}_x\text{Fe}_2\text{O}_4$), in comparison with monosubstituted ferrites, a higher initial rate of formation of the primary oxidation product of *m*-xylene — *m*-methylbenzylhydroperoxide (main intermediate product obtained during formation of *m*-toluic acid) is observed. The correlation of the activity of mono- and disubstituted Ni-Co ferrites, in the conditions of developed heterogeneous catalytic conversion of *m*-xylene, disubstituted Ni-Co ferrites are also characterized by higher rate of heterogeneous nucleation of free radicals and heterogeneous catalytic conversion of the intermediate product — *m*-toluic aldehyde to *m*-toluic acid. This, in turn, provides a high degree of selectivity for the targeted product with the yield of 79.8 %.

Keywords: nanodispersed catalysts, monoferrites, diferrites, solid-phase synthesis, natural magnetite, microwave radiation, liquid-phase oxidation, heterogeneous-catalytic conversion.

Introduction

The study of the heterogeneous catalytic liquid-phase oxidation patterns of alkyl aromatic compounds in the presence of metal compounds of variable valency is of great importance in the streamlined synthesis of the products of this reaction, which are mainly mono- and poly-carboxylic acids [1–8].

These compounds are of significant practical value for organic synthesis due to their functionality, for example, in the preparation of widely-used physiologically active substances and pharmaceuticals [9–11].

One of the effective methods for directing the above-mentioned liquid-phase process in the direction of high rate, conversion and selectivity to targeted products is the use of highly-dispersed (nano-sized) heterogeneous catalysts — complex metal oxides of variable valency [12–19].

In particular, due to such universal properties as high thermodynamic stability and corrosion resistance, mechanical hardness and high adsorption capacity, spinel-type ferrites with single and double displacement of Fe^{2+} and Fe^{3+} atoms with variable valence metals are of interest as potential heterogeneous catalysts of this type [20, 21].

The preceding studies [22, 23] present the results of microwave solid-phase synthesis of mono-substituted and double Ni–Co ferrites completed on the basis of $\text{Ni}^{(\text{II})}$, $\text{Co}^{(\text{II})}$ oxides and natural magnetite concentrate taken from the Dashkesan magnetite deposit (Gazakh economical region, Dashkesan city, Azerbaijan) and their initiating activity estimation in the reaction of liquid-phase oxidation of alkyl aromatic hydrocarbons.

It was found that a high initial formation rate of the primary product of *m*-xylene oxidation, *m*-methylbenzylhydroperoxide, a crucial product that determines the efficiency of further development of the reaction in the direction of the formation of *m*-toluic acid, is observed in the presence of samples with a spinel structure ($\text{Ni}_{1-x}\text{Co}_x\text{Fe}_2\text{O}_4$) formed under the thermal influence of microwave radiation, under conditions of an undeveloped radical-chain reaction.

A series of experiments were conducted to determine the activity of the synthesized catalysts. This article presents the results of the study of the heterocatalytic nucleation and continuation of chains in the initial period and during the period of the developed reaction of liquid-phase oxidation of *m*-xylene to *m*-toluic acid, in the presence of both monosubstituted Ni- and Co-ferrites, and ferrites of the composition $\text{Ni}_{0.6}\text{Co}_{0.4}\text{Fe}_2\text{O}_4$.

Experimental

As precursors for the solid-phase synthesis of nickel-cobalt mono- and di-substituted ferrites, divalent metal oxides MO: CoO (purity 99.9) and NiO (purity 99.9), *m*-xylene, as well as magnetite concentrate (Fe_3O_4) with an iron content of 70.4 % were used.

Prior to their heat treatment by microwave radiation the aforementioned oxides and magnetite were subjected to solid-phase interaction through simultaneous mechanical mixing in an electric agate mortar and pestle for 1 hour.

Thermal treatment of ferrite samples was carried out in an installation designed on the basis of a microwave oven EM-G5593V (Panasonic) with a resonator volume of 25 liters in the varying the magnetron power between 200–800 W with an operating frequency of 2450 MHz. The charge temperature was controlled with a CEM DT-8858 infrared pyrometer with a temperature measurement range of 50–1300 °C.

The conditions required for the formation of phase composition of the samples and their morphology are described in detail in [22, 23]. The samples used in this study were finely dispersed crystallites with linear dimensions in the range of 80–170 nm and a specific surface area of 11–63 m²/g which varied depending on the chemical composition.

Characteristics of metal oxides used in our work CoO (Purity 99.9, GOST 4467-79 Russia) and NiO (purity 99.9, GOST 4331-78 Russia), *m*-xylene (GOST 9410-78), magnetite concentrate Fe_2O_3 with 70 % (GOST 16589-86) are presented in [24–27].

The conversion of *m*-xylene was carried out in an installation combining a reaction unit — a bubble column with $d_{out} = 25$ mm, $h = 100$ mm with an external circulation circuit of gas flow ($\text{N}_2 + \text{O}_2$). The device design enabled carrying out the reaction both in the mode of stationary values of partial pressures of oxygen in the circulation circuit (flow-circulation mode) and in a continuously changing partial pressure of oxygen due to flow (or circulation) rate (circulation mode).

m-Xylene was converted in a solution of *o*-dichlorobenzene ($T_b = 179$ °C), which was inert to oxidative transformation under the experimental conditions. The inert diluent of the contacting air flow was nitrogen previously purified from oxygen impurities over a Cu/SiO₂ catalyst.

The partial pressure of oxygen in the circulating gas flow was also varied by introducing reduced O₂ from a gas-cylinder. The concentration of oxygen dissolved in the liquid phase was calculated using chromatographic technique for determination of the gas content in hydrocarbons [28] which is dependent on the partial pressure of oxygen in the bubbling gas flow.

The main part of the component composition of the liquid phase of the catalysts was identified by gas chromatographic analysis comparing the values of the retention volumes of the reaction products with those found for individual reactive products.

Quantitative analysis of gas-liquid chromatography was performed by the internal standard method (octanol-1 label) on an LKhM-80 MD device (3rd model) using a flame ionization detector with controlled heating of the column heating oven. Silicone SE-30, 10 % on a solid support of hezisorbe AWHMD was used as a stationary phase.

The concentration of carbon dioxide in the gaseous mixture at the outlet of the reactor was determined using a gas chromatograph (LKhM-80 MD device, detector — katharometer column, $l = 3.6$ m, $d_{out} = 3$ mm, filled with the “Porapak QS” phase) with controlled heating thermostat in the temperature range 30–65 with the rate of temperature elevation of 3/min. A mixture of oxygen and nitrogen was separated into individual components in the parallel column, $l = 1.2$ m, $d_{out} = 3$ mm, filled with NaX zeolite.

The carrier gas (He) rate in the columns was maintained within the range of 50–65 mL/min.

The content of *m*-methylbenzylhydroperoxide in the catalyzate was determined by iodometric titration of samples according to the technique described in [29] in the presence of starch as an indicator and was calculated using the formula:

$$\% \text{ hydroperoxide} = \frac{V \cdot M}{Q \cdot 200}, \quad (1)$$

where V — volume of 0.1N $\text{Na}_2\text{S}_2\text{O}_3$ solution used for titration of released iodine; M — molecule weight of hydroperoxide (137 atomic mass unit), Q — weighed sample of catalyzate.

In order to identify the dependence of the absorption rate of oxygen by the reaction medium on its concentration in the liquid phase, by special experiments, it was established that the dissolution isotherms of the oxygen in the reaction mixture in the region of observed linearity:

$$C_{\text{O}_2} = K_{\text{O}_2} \div P_{\text{O}_2}, \quad (2)$$

where $C_{\text{O}_2} \cdot 10^{-3}$, mol/L concentration of dissolved oxygen; K_{O_2} — solubility coefficient of O_2 in *m*-xylene at fixed temperature; P_{O_2} — partial pressure of oxygen in the gas flow, it was established that the temperature dependence of K_{O_2} coefficient is described by the following equation:

$$\lg K_{\text{O}_2} = -\frac{6500}{R \cdot T}, \quad (3)$$

here, 6500 is activation energy of dissolution of oxygen in *m*-xylene; R — universal gas constant $R = 8,314\,462\,618\,153\,24\text{ J}/(\text{mol} \cdot \text{K})$; T — temperature, K.

The rate of nucleation of free radicals was measured according to the following procedure. The rate of oxygen absorption (W_0) in the presence of the free radical inhibitor N,N'-di- β -naphthyl-*p*-phenylenediamine ($5.5 \div 6.0 \cdot 10^{-4}$ mol/L) introduced into the system during the reaction was calculated using the formula:

$$W_{\text{inh}} = \frac{2\Delta[\text{InH}]}{S \cdot \tau_{\text{inh}}}, \quad (4)$$

where W_{inh} — the inhibitor consumption rate ($\text{mol}/\text{m}^2 \text{ min}$), $\Delta[\text{InH}]$ — the amount of consumed inhibitor (mol); S — the surface area of the catalyst sample (m^2), 2 — the stoichiometric inhibition coefficient, τ_{inh} — the time period on the abscissa axis at extrapolation in coordinates $1/W_0 - \tau$ (Fig. 1). The moment of introduction of the inhibitor was taken as the beginning of the time coordinate. The consumption of the inhibitor was monitored by the accumulation of a colored product of its oxidation — di- β -naphthyl-*p*-quinonediimine, the concentration of which in selected catalytic samples was determined on an SF-4A spectrophotometer in regard to light wave absorption at $\lambda_{\text{max}} = 480\text{ }\mu\text{m}$ and molar extinction coefficient $\varepsilon = 1.1 \cdot 10^4\text{ L}/\text{mol} \cdot \text{cm}$.

Selectivity to targeted products was evaluated as ratio of yield of corresponding product to conversion of *m*-xylene to the total reaction products:

$$S_i (\text{wt. \%}) = \frac{Q_i}{\sum Q_i} \cdot 100, \quad (5)$$

where S_i — selectivity to targeted product of reaction; Q_i — weight of target products (g), Q_i — total amount of obtained products (g).

The statistical manipulation of the experimental results was ultimately aimed at determining the confidence interval boundary [29]:

$$\left[M - t_{n,p} \frac{S}{\sqrt{n}}; \quad M + t_{n,p} \frac{S}{\sqrt{n}} \right], \quad (6)$$

where M — average value of the data extraction; S — standard deviation; $t_{n,p}$ — table value of Student's distribution with a number of degrees of freedom (n) and confidence factor (P); n — number of elements in taken extraction of corresponding experiments.

Calculation was carried out using MS Excel (Windows 10) computational hardware and software in confidence level $P = 95\%$ and preliminary computation of the standard deviation (S), in $n = 3-4$ sample size.

Results and Discussion

The objective of the experiments was to ascertain whether the inhibitor could potentially impede the formation of free radicals. To this end, the initial rates of oxygen absorption were measured under conditions

where identical quantities of freshly prepared catalysts and catalysts filtered from a solution (5.5×10^{-4} mol/l) of the inhibitor, N,N'-di- β -naphthyl-p-phenylenediamine, were employed.

The experiments mentioned above, demonstrated that the amount of a chemisorbed inhibitor present was insufficient to impede the nucleation centers of free radicals on the surface of catalysts. Consequently the observed difference in oxygen absorption rates in the absence and presence of the inhibitor can be attributed to the interaction of the inhibitor and free radicals in the bulk liquid phases (Fig. 1).

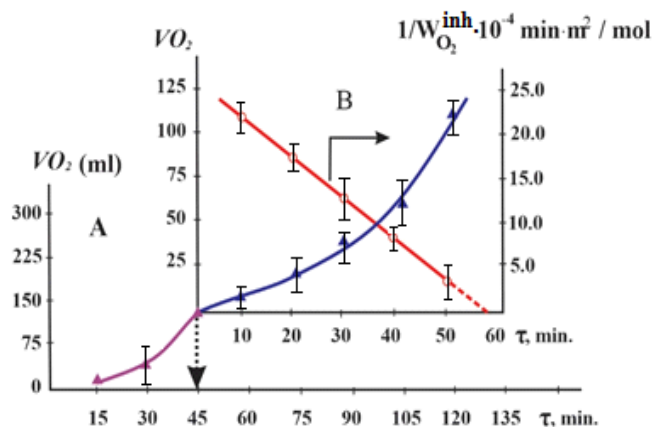


Figure 1. The kinetics of oxygen adsorption in the absence of an inhibitor (A), with the introduction of (5.5×10^{-4} mol/L) N,N'-di- β -naphthyl-p-phenylenediamine (B) (marked with an arrow) and the reciprocal value of the absorption rate of oxygen in the presence of a catalyst with the composition $\text{Ni}_{0.6}\text{Co}_{0.4}\text{Fe}_2\text{O}_4$. Temp. 413 K, the ratio of the catalyst surface area to the volume of the hydrocarbon phase (S/V) = $2 \cdot 10^5 \text{ m}^{-1}$. Confidence level $P = 95 \%$ and sample size $n = 3$

Experiments in which the initial rates of oxygen absorption were measured in the presence of identical loads of samples of freshly prepared catalysts and catalysts filtered from a N,N'-di- β -naphthyl-p-phenylenediamine solution (5.5×10^{-4} mol/L) showed the absence in noticeable quantities of the chemisorbed inhibitor capable of blocking the nucleation centers of the free radicals.

Figure 2 shows a histogram representing the dependence of the initial rate of heterogeneous catalytic chain initiation during the oxidation of *m*-xylene in the presence of synthesized Ni-Co ferrites and the conversion rate which does not exceed 3–5 %. At this conversion rate the formation of free radicals by hydroperoxide branching of chains and, consequently, the effect of the radicals on the kinetics of the radical chain process can be disregarded.

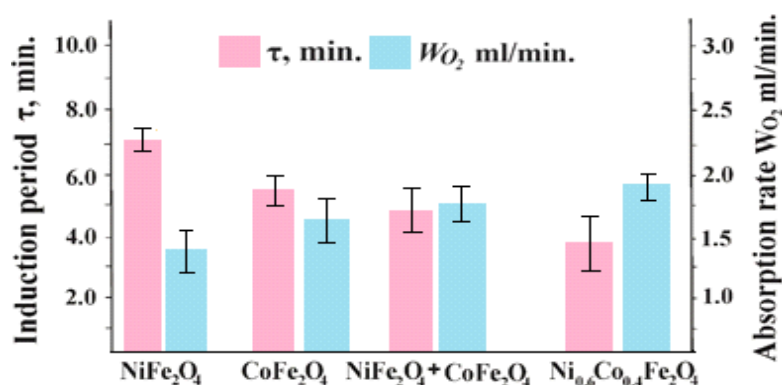


Figure 2. Dependence of the induction period (τ) and the initial absorption rate of oxygen (W_{O_2}) in the presence of synthesized catalysts in the liquid-phase oxidation of *m*-xylene. Conditions: Temperature 403 K; the weight concentration of catalysts is 2.5 %. Confidence level $P = 95 \%$ and sample size $n = 3, 4$.

The initiating activity data of the synthesized double Ni-Co ferrites were compared with the activities of mono-substituted samples, as well as a mechanical mixture of ferrites ($\text{NiFe}_2\text{O}_4 + \text{CoFe}_2\text{O}_4$) taken in a mass ratio of 1:1.

It has been established that the introduction of the inhibitor at the starting moment of the reaction does not result in complete inhibition of oxygen absorption, and this fact is not due to the insufficient efficiency of the used inhibitor, but is associated with the presence of uninhibited heterogeneous catalytic conversion pattern of xylene. Among the tested samples, spinel samples with the composition $\text{Ni}_{0.6}\text{Co}_{0.4}\text{Fe}_2\text{O}_4$ are characterized by the shortest induction period and the highest initial rate of oxygen absorption.

The dependence of the induction period and the rate of oxygen absorption on the time of introduction of the inhibitor into the oxidized *m*-xylene at different ratios of the total value of the heterogeneous surface to the volume of *m*-xylene charged into the reactor (S/V) was studied in order to clarify the role of the active surface of the $\text{Ni}_{0.6}\text{Co}_{0.4}\text{Fe}_2\text{O}_4$ catalyst and the volumetric transformations of *m*-xylene in the stage of nucleation of primary xylyl radicals.

It can be seen in Figure 3 that with an increase in the S/V ratio the amount of the introduced catalyst increases, a more intense decay of the induction period is observed starting from the time of introduction of the inhibitor.

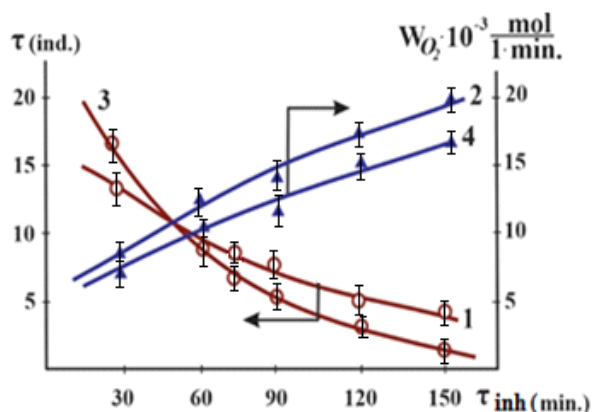


Figure 3. Dependence of the induction period and the rate of oxygen absorption on the time of introduction of the inhibitor during the conversion of *m*-xylene in the presence of the catalyst $\text{Ni}_{0.6}\text{Co}_{0.4}\text{Fe}_2\text{O}_4$; and the value of the rate of oxygen absorption at the time of introduction of the inhibitor. (1 and 2) — $S/V = 31.4 \cdot 10^5 \text{ m}^{-1}$; (3, 4) — $15.7 \cdot 10^5 \text{ m}^{-1}$. (Conditions: temp. 403K, $p = 0.25 \text{ at.}$; $V_{m\text{-xyl.}} = 40 \text{ mL}$, $V_{\text{gas}} = 35 \text{ L/h}$). Confidence level $P = 95 \%$ and sample size $n = 3-4$

In this case, there is also a more intense increase in the absorption rate of oxygen measured at the time of introduction of the inhibitor.

This phenomenon can be attributed to the heterogeneous catalytic nucleation of free xylyl radicals during the interaction of the converted *m*-xylene with the active surface of the $\text{Ni}_{0.6}\text{Co}_{0.4}\text{Fe}_2\text{O}_4$ catalyst.

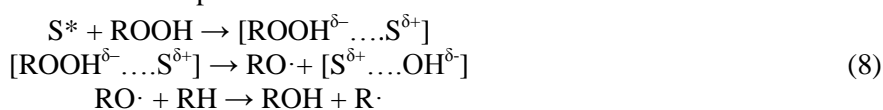
At the same time, a more intense decay of the induction period is observed starting from the time of introduction of the inhibitor during the period of the developed reaction.

This indicates an increase in the proportion of the branched chain mechanism in the formation process of free radicals, which occurs in the bulk of the liquid phase of oxidized *m*-xylene in the presence of a less catalyst sample by mass (Fig. 3).

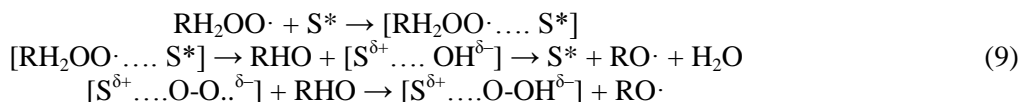
As is known, the composition of hydrocarbon oxidation products, including alkyl aromatic compounds, is determined by various directions of conversions of the primarily formed peroxide radicals $\text{ROO}\cdot$. During conversion in the bulk of the liquid phase, the main direction of the homogeneous chain continuation reaction is the interaction of the initial hydrocarbon with the formation of hydroperoxides [30–35]:



The decomposition of hydroperoxides catalyzed by the heterogeneous surface usually leads to the formation of the corresponding alcohols as molecular products:



As an alternative reaction of chain continuation may involve the interaction of peroxide radicals with active centers located on the surface of the catalysts resulting in the formation of aldehydes:



Analysis of the composition of the catalyzate in the initial and subsequent periods of the reaction proceeding in the presence of mono- and di-substituted ferrites showed that the selectivity to *m*-methylbenzyl alcohol increases (Tables 1, 2) in cobalt ferrite with a relatively low specific surface area.

Table 1

Conversion of *m*-xylene in the presence of mono- and di-substituted ferrites of Co and Ni
(Conditions: Temp. 403 K; $V_{m\text{-xylene}} = 40 \text{ ml}$; v air flow 35 L/h)

S/V M ⁻¹ ×10 ⁵	τ, reaction time, min	Conver- sion of <i>m</i> -xylene, %	Selectivity to reaction products % (wt.) (± Confidence interval with Student's distribution in α = 0.05)				
			Hydroperoxide of <i>m</i> -methyl benzele	<i>m</i> -methyl- benzyl alcohol	<i>m</i> -toluic aldehyde	<i>m</i> -toluic acid	<i>i</i> -phthalic acid
NiFe ₂ O ₄ (S _{sp. sur.} = 23 m ² /g)							
5.75	20	4.2 ±0.7	3.7±0.7	31.5±0.8	46.5±0.7	18.3±0.5	—
5.75	60	15.8±0.6	2.3±0.8	13.2±0.3	44.8±0.6	39.7±0.5	—
5.75	120	51.6±0.8	1.8±0.6	8.8±0.9	27.2±0.8	60.6±0.4	1.6±0.8
CoFe ₂ O ₄ (S _{sp. sur.} = 11 m ² /g)							
2.75	20	3.4±0.5	4.2±0.5	32.8±0.6	47.3±0.2	15.7±0.4	—
2.75	60	14.4±0.3	2.8±0.6	14.6±0.4	42.3±0.5	38.9±0.3	1.4±0.9
2.75	120	47.7±0.2	2.2±0.8	10.6±0.6	23.8±0.6	59.7±0.2	3.7±0.5
Ni _{0.6} Co _{0.4} Fe ₂ O ₄ (S _{sp. sur.} = 63 m ² /g)							
15.70	20	6.3±0.8	2.8±0.7	15.6±0.5	48.4±0.2	33.2±0.3	—
15.70	60	27.2±0.5	1.6±0.8	10.8±0.7	32.8±0.5	53.1±0.2	1.7±0.8
15.70	120	68.6±0.2	0.8±0.9	5.4±0.8	19.4±0.6	70.2±0.2	4.2±0.6

* $S_{\text{sp. sur.}}$ — Specific surface area of the catalyst.

Table 2

Conversion of *m*-xylene in the presence of mono- and di-substituted ferrites of Co and Ni
(Conditions: Temp. 413 K; $V_{m\text{-xylene}} = 40 \text{ ml}$; v air flow 35 L/h)

S/V M ⁻¹ ×10 ⁵	τ, reac- tion time, min	Conver- sion of <i>m</i> -xylene, %	Selectivity to reaction products % (wt.) (± Confidence interval with Student's distribution in α = 0.05)				
			Hydroperoxide of <i>m</i> -methyl benzele	<i>m</i> -methyl benzyl alcohol	<i>m</i> -toluic aldehyde	<i>m</i> -toluic acid	<i>i</i> -phthalic acid
NiFe ₂ O ₄ (S _{sp. sur.} = 23 m ² /g)							
5.75	20	6.8±0.6	3.2±0.7	28.7±0.5	37.5±0.3	30.6±0.3	—
5.75	60	25.3±0.5	1.8±0.8	10.2±0.5	35.6±0.4	52.4±0.3	—
5.75	120	54.2±0.5	1.3±0.8	6.4±0.3	22.3±0.4	67.2±0.2	2.8±0.8
CoFe ₂ O ₄ (S _{sp. sur.} = 11 m ² /g)							
2.75	20	6.2±0.5	3.4±0.5	30.4±0.2	42.5±0.4	23.7±0.5	—
2.75	60	34.4±0.3	2.4±0.6	12.3±0.5	37.4±0.5	45.4±0.3	2.5±0.7
2.75	120	49.6±0.3	1.7±0.5	8.8±0.5	21.4±0.5	63.8±0.2	4.3±0.6
Ni _{0.6} Co _{0.4} Fe ₂ O ₄ (S _{sp. sur.} = 63 m ² /g)							
15.70	20	10.3±0.4	1.7±0.6	10.2±0.3	37.8±0.2	50.3±0.3	—
15.70	60	37.4±0.3	1.2±0.7	7.6±0.5	22.6±0.5	64.9±0.2	3.7±0.6
15.70	120	75.3±0.2	0.5±0.9	3.8±0.6	9.7±0.6	79.8±0.3	6.2±0.5

This fact can be interpreted as evidence for the predominance of the hydroperoxide mechanism of chain continuation in the presence of cobalt monoferrite. In this case, as illustrated in Figure 2, the rate of chain continuation in the bulk liquid phase with the participation of *m*-methylbenzylhydroperoxide (Scheme 8) is greater than the rate of chain continuation with the participation of *m*-toluylaldehyde (Scheme 9) during the period of the developed reaction.

Assuming that the formation process of the free radicals is determined by the stage of heterogeneous catalytic initiation of chains under conditions of an undeveloped chain reaction. Consequently it may be possible to estimate the rate of this process in the form of the difference between the rate of oxygen absorption in the presence of the inhibitor and the rate of chain inhibition:

$$W_R = -W_{\text{inh}} \quad (10)$$

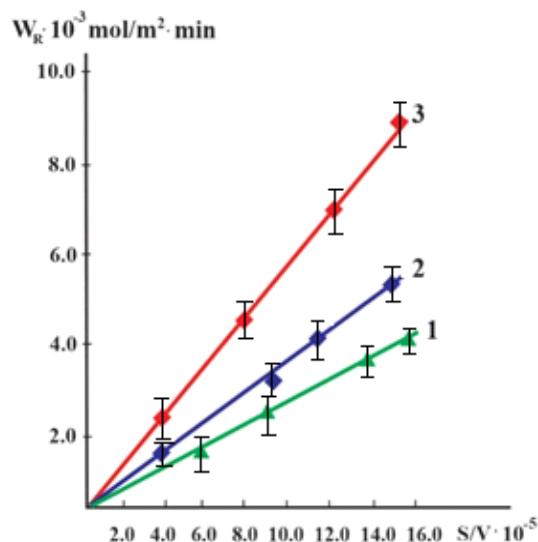
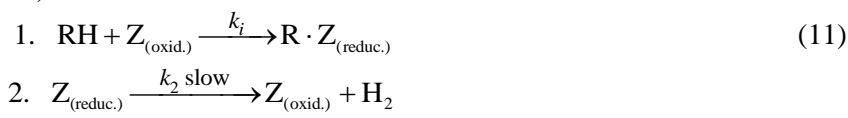


Figure 4. Dependence of the initial rate of heterogeneous catalytic initiation of chains on the surface of NiFe₂O₄ (1); CoFe₂O₄ (2) and Ni_{0.6}Co_{0.4}Fe₂O₄ (3) samples on the ratio of their total surface area to the initial volume of *m*-xylene (S/V), which is variable by changing the catalyst loading; Conditions: reaction temperature 413K, volume of loaded *m*-xylene; 40 mL, *v* air flow 35 L/h. Confidence level *P* = 95 % and sample size *n* = 3

The observed proportionality of W_R to the amount can be explained by the following scheme of free radical formation during the interaction of *m*-xylene with active centers on the heterogeneous surface of the catalyst (it is assumed that step 2 is slow):



where $\text{Z}_{(\text{oxid.})}$ — oxidized center, $\text{Z}_{(\text{reduc.})}$ — reduced center located on the surface of the catalyst.

The results presented in Tables 1 and 2, demonstrate that the catalysts are involved in the initiation and continuation of reaction chains, as well as in the formation of oxygen-containing molecular reaction products in the heterocatalytic liquid-phase oxidation process of *m*-xylene in the presence of both mono- and di-substituted ferrites.

It was established that, based on a set of parameters including the selectivity towards the targeted product — *m*-toluic acid, di-substituted Ni–Co ferrites exhibited an advantage under comparable reaction conditions by a relatively high rate of heterogeneous nucleation of free radicals and further heterogeneous catalytic conversion of the intermediate product — *m*-tolualdehyde into *m*-toluic acid.

Conclusions

Summarizing the results of the research, we can state that mono- and di-substituted nickel and cobalt ferrites synthesized by microwave solid-phase synthesis, particularly samples of the Ni_{0.6}Co_{0.4}Fe₂O₄ composition with a spinel structure, are characterized by higher rate of oxygen adsorbed by the reaction system in the initial period and in the period of the developed reaction of liquid-phase oxidation of *m*-xylene to *m*-toluic acid.

The high rate of heterogeneous catalytic conversion of the intermediate reaction product — *m*-toluic aldehyde into *m*-toluic acid provides the high selectivity to the targeted product of the process.

Author Information*

*The authors' names are presented in the following order: First Name, Middle Name and Last Name

Nargalam Muzaffar gizi Hasanguliyeva — PhD in Chemistry, Leading Researcher, Institute of Catalysis and Inorganic Chemistry named after acad. M. Nagiyev of Ministry of Science and Education of the Republic of Azerbaijan, Ave. H. Javid 113, Az 1143, Baku, Azerbaijan; e-mail: nqasanquliyeva@mail.ru; <https://orcid.org/0000-0003-4709-238x>

Ninel Vladislavovna Shakunova (corresponding author) — PhD in Chemistry, Senior Researcher, Institute of Catalysis and Inorganic Chemistry named after acad. M. Nagiyev of Ministry of Science and Education of the Republic of Azerbaijan, Ave. H. Javid 113, Az 1143, Baku, Azerbaijan; e-mail: shakunova_ninel@mail.ru; <https://orcid.org/0000-0002-9218-6839>

Yuriy Nikolaevich Litvishkov — Doctor of Chemistry, Professor, Corresponding Member of ANAS, Institute of Catalysis and Inorganic Chemistry named after acad. M. Nagiyev of Ministry of Science and Education of the Republic of Azerbaijan, Ave. H. Javid 113, Az 1143, Baku, Azerbaijan; e-mail: yuriylit@rambler.ru; <https://orcid.org/0000-0003-0662-1257>

Author Contributions

All authors contributed to the preparation of the manuscript. All authors approved the final version of the manuscript. **CRedit**: **Nargalam Muzaffar gizi Hasanguliyeva** — conducting research, obtaining data, analyzing results, data manipulation, writing an article; **Ninel Vladislavovna Shakunova** — experimentation, data manipulation, text processing; **Yuri Nikolayevich Litvishkov** — conceptual development, research methodology, editing, approval of the final version of the article.

Conflicts of Interest

The authors declare no conflict of interest.

Acknowledgments

Authors express their gratitude to the management of the institute and all organizational structures — the library, the analytical department for providing assistance for the compilation of the article.

References

- 1 Sokolova, V.V., Naymushina, I.V., Sadikova, A.N., Mantabayeva, A.A., Tashmukhambetova, J.Kh., & Kairbekov, J.K. (2012). Polimerno-immobilizovannyye kompleksi kobalta (II), nanesennyye na steklo, kak katalizatory protsessy oksigenatsii toluola. [Polymer-immobilized cobalt (II) complexes deposited on glass as catalysts for the process of oxygenation of toluene]. *Aktualnye problemy gumanitarnykh i estestvennykh nauk — Current problems of humanities and natural sciences*, 7 (42), 18–23 [in Russian].
- 2 Buxarkina, T.V., Verzhitsinskaya, S.V., Fedyushkina, A.Q., Belousov, Yu.A., & Borisov, Yu.A. (2020). Poluchenie aromatischeskikh kislot zhidkofaznym okisleniem uglevodorodov. [Preparation of aromatic acids by liquid-phase oxidation of hydrocarbons]. *Nauchnyi zhurnal Rossiyskogo gazovogo obshchestva — Scientific Journal of the Russian Gas Society*, 1(24), 28–37 [in Russian].
- 3 Tsang, S.C., Zhu, J., & Yu, K.M.K. (2006). Selective catalytic oxidation of alkylaromatic molecules by nanosize water droplets containing Co^{2+} species in supercritical carbon dioxide fluid. *Journal of Experimental Nanoscience*, 1(4), 435–456. <https://doi.org/10.1080/17458080601067682>
- 4 Shangareev, D.R., Antonova, T.N., Abramov, I.G., Sivova, T.S., & Danilova, A.S. (2021). Catalytic Liquid-Phase Oxidation of Cyclooctene to 1,2-Epoxyoctane Using Molecular Oxygen. *Kinetics and Catalysis*, 62(1), 98–102. <https://doi.org/10.1134/s0023158421010080>
- 5 Digurov, N.G., Bukharkina, T.V., Verzhichinskaya, S.V., & Makarov, M.Y. (2010). Liquid-phase oxidation of ethylbenzene with air oxygen in the presence of a mixed cobalt-manganese catalyst. *Oil and Gas Technologies (scientific and technological journal)*, 3, 31–36.
- 6 Lebedeva, N.V., Koshel, G.N., & Koshel, S.G. (2020). Liquid Phase Catalytic Oxidation 3,5-Xylenol. *Izvestiya Vysshikh Uchebnykh Zavedeniy Khimicheskaya Tekhnologiya — News of Higher Educational Institutions Chemistry Chemical Technology*, 63(3), 4–9. <https://doi.org/10.6060/ivkkt.20206303.6095>
- 7 Shakunova, N.V., Zulfuqarova, S.M., Aleskerova, Z.F., Faradjev, Q.M., & Litvishkov, Yu.N. (2005). Nekotorye zakonomernosti zhidkofaznogo okisleniya m-ksilola v prisuststvi katalizatorov Co-Mn/Al₂O₃/Al-karkas. [Some regularities of liquid-phase oxidation of m-xylene in the presence of Co-Mn/Al₂O₃/Al-framework catalysts]. *J. Neftepererabotka i neftekhimiya — J. Oil Refining and Petrochemistry*, 12, 21–23 [in Russian].

- 8 Lyu, Q., Dong, J., He, R., Sun, W., & Zhao, L. (2021). Modeling of the Co-Mn-Br catalyzed liquid phase oxidation of *p*-xylene to terephthalic acid and *m*-xylene to isophthalic acid. *Chemical Engineering Science*, 232, 116340. <https://doi.org/10.1016/j.ces.2020.116340>
- 9 Brel, A.K., Lisina, S.V., Budayeva, Yu.N., & Rodina, N.V. (2013). Sintez i psikhotropnye svoystva solei N-(4-gidroksibenzoil)glitsina i N-(4-atsetoksibenzoil)glitsina. [Synthesis and psychotropic activity of N-(4-hydroxybenzoyl)glycine and N-(4-acetoxybenzoyl)glycine salts]. *Fund. Issled. — Fundamental research*, 10, Pt9, 1963–1967 [in Russian].
- 10 Gritsenko, I.S., Taran, S.Q., & Isaev, S.Q., et al. (2014). Lekarstvennye sredstva alifaticheskoi i aromatischeskoi struktury: lektzii po farmatsevticheskoi khimii dlia studentov farmatsevticheskikh fakul'tetov vysshikh uchebnykh zavedenii III–IV urovnei akkreditatsii [Medicines of aliphatic and aromatic structure: lectures on pharmaceutical chemistry for students of pharmaceutical faculties of higher educational institutions of III–IV levels of accreditation]. *Khim. Izdatel'stvo NUF. — Chemical Publishing house NUPh*, 147 [in Russian].
- 11 Aristanova, T.A. (2022). Farmatsevticheskaiia khimiia [Pharmaceutical chemistry]. Almaty: Medet Group. — Almaty: «Medet Group», T.2. 524 [in Russian].
- 12 Knobl, S. (2003). The synthesis and structure of a single-phase, nanocrystalline MoVW mixed-oxide catalyst of the Mo₅O₁₄ type. *Journal of Catalysis*, 215(2), 177–187. [https://doi.org/10.1016/s0021-9517\(03\)00006-x](https://doi.org/10.1016/s0021-9517(03)00006-x)
- 13 Litvishkov Yu.N., Zulfugarova S.M., Shakunova N.M., & Aleskerova Z.F. (2004). Zhidkofaznoe okislenie *m*-ksilola v prisutstvii karkasnogo katalizatora Co-Mn/Al₂O₃/Al. [Liquid-phase oxidation of *m*-xylene in presence of Co-Mn/Al₂O₃/Al framework catalyst]. *Azerbaidzhanskii khimicheskii zhurnal — Azerbaijan Chemistry Journal*, 4, 22–26 [in Russian].
- 14 Litvishkov, Yu.N., Tretyakov, V.F., Talishinskaya, P.M., Shakunova, N.M., Zulfugarova, S.M., Aleskerova, Z.F., Mardanova, N.M., & Kashkay, A.M. (2013). Mikrovolnovaia intensivatsiia geterogenno-kataliticheskoi zhidkofaznoi reaktsii okisleniia *m*-ksilola v prisutstvii nanostrukturirovannogo katalizatora Co-Mn/Al₂O₃/Al. [Microwave intensification of heterogeneous catalytic liquid-phase oxidation reaction of *m*-xylene in the presence of nanostructured-Co-Mn/Al₂O₃/Al catalyst]. *Nanotekhnologii: nauka i proizvodstvo. — Nanotechnology: science and production*, 1(22), 15–22 [in Russian].
- 15 Masood, Z., Ikhlaiq, A., Akram, A., Qazi, U. Y., Rizvi, O. S., Javaid, R., Alazmi, A., Madkour, M., & Qi, F. (2022). Application of Nanocatalysts in Advanced Oxidation Processes for Wastewater Purification: Challenges and Future Prospects. *Catalysts*, 12(7), 741. <https://doi.org/10.3390/catal12070741>
- 16 Majeed Ahmed, L. (2021). Bulk and Nanocatalysts Applications in Advanced Oxidation Processes. *Oxidoreductase*, 7, 107–111. <https://doi.org/10.5772/intechopen.94234>
- 17 Avramenko, V.A., Bratskaya, S. Yu., Karpov, P.A., Mayorov, V. Yu., Mironenko, A.Yu., Palamarchuk, M.S., & Sergienko, V.I. (2010). Macroporous catalysts for liquid-phase oxidation on the basis of manganese oxides containing gold nanoparticles. *Doklady Physical Chemistry*, 435(2), 193–197. <https://doi.org/10.1134/s0012501610120018>
- 18 Ahmed, L.M., Ivanova, I., Hussein, F.H., & Bahnmann, D.W. (2014). Role of Platinum Deposited on TiO₂ in Photocatalytic Methanol Oxidation and Dehydrogenation Reactions. *International Journal of Photoenergy*, 1–9. <https://doi.org/10.1155/2014/503516>
- 19 Krumova, K., & Cosa, G. (2016). Chapter 1. Overview of Reactive Oxygen Species. *Comprehensive Series in Photochemical & Photobiological Sciences*, 1–21. <https://doi.org/10.1039/978178262208-00001>
- 20 Kharisov, B.I., Dias, H.V.R., & Kharissova, O.V. (2019). Mini-review: Ferrite nanoparticles in the catalysis. *Arabian Journal of Chemistry*, 12(7), 1234–1246. <https://doi.org/10.1016/j.arabjc.2014.10.049>
- 21 Kaur, M., & Kaur, N. (2016). Ferrites: Synthesis and Applications for Environmental Remediation. *Ferrites and Ferrates: Chemistry and Applications in Sustainable Energy and Environmental Remediation*, 113–136. <https://doi.org/10.1021/bk-2016-1238.ch004>
- 22 Litvishkov, Yu.N., Zulfugarova, S.M., Aleskerova, Z.F., Gasanguliyeva, N.M., Shakunova, N.V., & Aleskerov, A.G. (2018). Microwave Synthesis of Co, Ni, Cu, Zn Ferrites. *Russian Journal of Applied Chemistry*, 91(5), 793–801. <https://doi.org/10.1134/s1070427218050105>
- 23 Hasanguliyeva, N.M., Shakunova, N.M., Litvishkov, Yu.N., Samedova, R.A. (2023). Mikrovolnovoi sintez ferritov Ni-Co i ikh initsiiruyushchaya aktivnost v zhidkofaznom okislenii alkilaromaticeskikh uglevodorodov. [Microwave synthesis of Ni-Co ferrites and their initiating activities in liquid-phase oxidation of alkyl aromatic hydrocarbons]. *Neftepererabotka i neftekhimiia — Oil Refining and Petrochemistry*, 9, 38–44 [in Russian].
- 24 GOST 4467–79. (1979). Reaktivy. Kobalt (II, III) oksid. Tekhnicheskie usloviia [Reagents. Cobalt (II, III) oxide. Specifications]. *Gosudarstvennyi standart SSSR — State standard of the USSR* [in Russian].
- 25 GOST 4331-78. (1980). Reaktivy. Nikelia okis chernaia. Tekhnicheskie usloviia [Reagents. Nickel black oxide. Specifications]. *Gosudarstvennyi standart SSSR — State standard of the USSR* [in Russian].
- 26 GOST 9410-78. (1980). Ksilol neftianoi. Tekhnicheskie usloviia [Petroleum xylol. Specifications]. *Gosudarstvennyi standart SSSR — State standard of the USSR*. [in Russian]
- 27 GOST 16589–86. (1988). Rudy zheleznye tipa zhelezistykh kvartsitov. Metod opredeleniia zheleza magnetita [Iron ores of iron quartzite type. Method for determination of magnetite iron]. *Gosudarstvennyi standart SSSR — State standard of the USSR* [in Russian].
- 28 Budanov, V.V., & Lefedova, O.V. (2011). Kineticheskie modeli zhidkofaznykh reaktsii [Kinetic models of liquid-phase reactions]. *Uchebnoe posobie, Ivanovo — Study guide, Ivanovo*. 177 [in Russian].
- 29 Antanovskiy, V.L., & Khursan, S.L. (2003). Fizicheskaiia khimiia organicheskikh peroksidov [Physical chemistry of organic peroxides]. Moscow: Akademkniga — Moscow: Academic book, 391 [in Russian].

-
- 30 Guo, B., & Yuan, Y. (2015). A comparative review of methods for comparing means using partially paired data. *Statistical Methods in Medical Research*, 26(3), 1323–1340. <https://doi.org/10.1177/0962280215577111>
- 31 Bach, R.D., Ayala, P.Y., & Schlegel, H.B. (1996). A Reassessment of the Bond Dissociation Energies of Peroxides. An ab initio Study. *Journal of the American Chemical Society*, 118(50), 12758–12765. <https://doi.org/10.1021/ja961838i>
- 32 Exner, O. (1983). Stereochemical and conformational aspects of peroxy compounds. *Peroxides*, 85–96. Portico. <https://doi.org/10.1002/9780470771730.ch2>
- 33 Rossiter, B.E., & Frederick, M.O. (2013). Triphenylmethyl Hydroperoxide. *Encyclopedia of Reagents for Organic Synthesis*. <https://doi.org/10.1002/047084289x.rt363m.pub2>
- 34 Matsui, K. (2006). Green leaf volatiles: hydroperoxide lyase pathway of oxylipin metabolism. *Current Opinion in Plant Biology*, 9(3), 274–280. <https://doi.org/10.1016/j.pbi.2006.03.002>
- 35 Noyori, R., Aoki, M., & Sato, K. (2003). Green oxidation with aqueous hydrogen peroxide. *Chemical Communications*, 16, 1977. <https://doi.org/10.1039/b303160h>